Preprints of the 19th World Congress
The International Federation of Automatic Control
Cape Town, South Africa. August 24-29, 2014

Comparison of different solutions in predictive control for two PMSM in parallel

MAURICE FADEL [1,2], ANA LLOR [1,2]

[1] LAboratoire PLAsma et Conversion d'Energie - LAPLACE

UMR 5213, CNRS, INPT, UPS : 2 rue Camichel BP7122 - 31071 Toulouse Cedex7, France
[2]CNRS; LAPLACE; F-31062 Toulouse, France.
fadel, llor, @laplace.univ-tlse.fr

Abstract: **This study concerns the power supply in parallel of 2 Permanent Magnet Synchronous Machines (PMSM) with the same inverter, in order to reduce the mass of embedded systems. This operation requires information from the two machines to ensure the stability of the system. Today several solutions address this objective, but about to improve energy efficiency it is important to develop new algorithms. The classical approach is based on a master-slave procedure where the current is controlled only in a master machine and the slave machine is simply connected in parallel. This solution guarantees stability but losses are not minimal. Predictive control applied to this configuration helps to ensure the stability of the system and gives the possibility to reduce Joule losses. In this way 3 predictive control laws are proposed by setting appropriated criteria. The first law uses the concept of master-slave machine, the second is defined with a criterion taking into account the two machines and the third uses the concept of virtual vectors which leads to an implementation of Space-Vector Pulse Width Modulation (SV-PWM). Results are compared in terms of dynamic performances and losses. The algorithms are tested on an experimental low-power test-bench.**

Keywords: **PMSM; Finite Control State-Model Predictive Control (FCS-MPC); SV-PWM; Dual Machine**

I. INTRODUCTION

Today the Permanent Magnet Synchronous Machine (PMSM) is a high performance actuator used both for its dynamic performances and for its energy performances [19]. Therefore, this machine is preferentially used in the field of aeronautics. Overall, for embedded systems, it appears today other specific needs for actuators working in cooperation, i.e. when 2 or more actuators are combined to achieve the same objective. This is the case, for example, of the flaps on the aircraft wings to do a synchronized development of flight surfaces, even when both load torques are different. This is also the case for braking applications, using different actuators distributed and synchronized to a common goal. So, as soon as it concerns the association of several actuators for a same function, it seems reasonable to limit the number of static converters embedded, in order to reduce the weight and volume of the system. This is the context of our work, which considers two PMSM supplied from the same three-phase voltage inverter.

The intensive use of the synchronous machine as an actuator is also related to the autopilot operation, ensuring a rigid link between the rotation frequency and rotation speed [19]. This procedure uses a position encoder and ensures the stability of the machine even under sudden torque impacts. Unlike asynchronous machines, parallel connected synchronous machines can present stability problems, since only one machine can be auto-piloted at a time. One solution, protected by a patent [1], [3], has already been found. It is a strategy type Master-Slave to define at each moment the machine which will be controlled (Master machine), while the second is just connected in parallel (Slave). If the stability is guaranteed, then it can be interesting to consider the question of energy efficiency and performance of this solution. Indeed, when a single machine is considered, the degrees of freedom of the power inverter allow imposing any desired torque by reducing the consumed current [16]. It is difficult to maintain this property when the inverter feeds two machines, and losses can become important. Therefore, the deal is to search control laws ensuring the stability of the two machines, in order to reduce the energy consumption. The solution is found, based in a compromise because supply voltages provided by the power inverter cannot be optimal for both machines at the same time, if their load torques are different. In this work we will work with a particular control type, which is the Finite Control Set-Model Predictive Control (FCS-MPC). The predictive control is based on a prediction model providing the currents evolution on the d-q axes, for all possible combinations of the inverter switches [10]. The best combination, evaluated using a criterion, is then retained and applied during the next sampling period. The criterion constitutes an arbitration to choose one alternative among all candidate solutions. It is on the choice of the criterion where we have focused our efforts, by comparing different possibilities, taking into account this particular system containing two machines. Three control laws (CL), which considers three different criteria, will be evaluated and compared:

> CL1: only the master machine (chosen from stability considerations) is evaluated in the cost function. The best the sum of the squares of d-q current errors.

> CL2: one criterion is used for both machines, containing the sum of the squares of both, d-axis and q-axis current errors for both machines.

> CL3: based in the CL2 method, but the selected vector is used as a basis to consider a finite number of virtual vectors which will be evaluated to minimize the criterion. The selected voltage vector is applied via a SV-PWM technique.

In section II the FCS-MPC method is presented for only one PMSM. Section III develops the model for the complete considered system (2 PMSM connected in parallel). Also the details of the three compared control criteria are given. In section IV it is presented the test procedure for the comparison process. Section V shows experimental results and the three control laws are then compared in terms of quality of response and Joule losses. The quality of the response is evaluated through the squared error of (d,q) axes currents.

II. FCS-MPC FOR ONE PMSM

The FCS-MPC introduced several years ago, is very well adapted to conversion energy devices, as static converters [13], [19]. We consider here the PMSM powered by a three phase inverter represented in figure 1. In this paper we consider a non-salient pole PMSM through a speed control application.

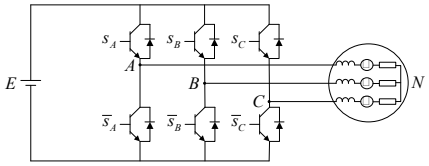

Fig. 1. Three-phase structure of the converter-machine association.

A two-level three-phase inverter has a finite number of possible control configurations. The 8 different control states of the inverter are represented in TABLE I. Configurations 0 and 7 are identical in terms of output voltage, so onwards only the combination 7 will be considered.

	0	1	2	3	4	5	6	7
S_A	**0**	**1**	**1**	**0**	**0**	**0**	**1**	**1**
S_B	**0**	**0**	**1**	**1**	**1**	**0**	**0**	**1**
S_C	**0**	**0**	**0**	**0**	**1**	**1**	**1**	**1**

TABLE I: Inverter configurations

To select the most appropriate vector, an optimal control problem must be solved after definition of a criterion of satisfaction. The voltage vector minimizing this criterion should then be chosen to be applied. The predictive model must be the most accurate possible to predict the future behavior of the system when applying a control combination of the inverter [7].

A. Model of PMSM (Permanent Magnet Synchronous Machine)

Considering that the magnetic circuit operates in linear regime, the electromotive force is sinusoidal and the magnetic losses and the cogging torque are negligible. Equations of the electrical machine in the d-q frame are expressed as follows:

$$u_d = R_s i_d + L\frac{d\Psi_d}{dt} - \omega_e \Psi_q \quad (1)$$

$$u_q = R_s i_q + L\frac{d\Psi_q}{dt} + \omega_e \Psi_d \quad (2)$$

With:

$$\Psi_d = L i_d + \Psi_f \quad (3)$$

$$\Psi_q = L i_q \quad (4)$$

Where u_d, u_q, i_d, i_q, L Ψ_d and Ψ_q represent, respectively, the voltages and stator currents, synchronous inductance and flux in the d-q axes. Ψ_f is the flux generated by the permanent magnets, R_s the stator resistance, $\omega_e = n_p.\omega_r$ (where ω_r is the rotor speed) and n_p the number of pole pairs. The electromagnetic torque is given by equation (5), and the speed by equation (6).

$$T_e = \frac{3}{2} n_p \left(\Psi_d i_q - \Psi_q i_d\right) = \frac{3}{2} n_p \Psi_f i_q \quad (5)$$

$$T_e - T_L = J\frac{d\omega_r}{dt} + f\omega_r \quad (6)$$

$$\frac{d\Theta_r}{dt} = \omega_r \quad (7)$$

J represents the inertia of the rotor, f the coefficient of viscous friction, T_L the load torque and θ_r the rotor position. With a low switching period we can consider that during that period the speed remains constant. In this case, the discrete model of the synchronous machine can be expressed as presented in equation (8), where T_s represents a sampling time:

$$\begin{bmatrix} i_d(k+1) \\ i_q(k+1) \end{bmatrix} = \begin{bmatrix} 1 - T_s\frac{R_s}{L} & T_s\omega_e(k) \\ -T_s\omega_e(k) & 1 - T_s\frac{R_s}{L} \end{bmatrix} \begin{bmatrix} i_d(k) \\ i_q(k) \end{bmatrix} + \begin{bmatrix} \frac{T_s}{L} & 0 \\ 0 & \frac{T_s}{L} \end{bmatrix} \begin{bmatrix} u_d(k) \\ u_q(k) \end{bmatrix} + \begin{bmatrix} 0 \\ T_s\frac{\omega_e(k)}{L} \end{bmatrix} \Psi_f \quad (8)$$

Thus the prediction of the torque can be achieved by (9):

$$T_e(k+1) = \frac{3}{2} n_p \Psi_f i_q(k+1) \quad (9)$$

B. Three-phase inverter model

A 2-level 3-phase inverter is used to feed the machine. The mathematical model is given by equation (10).

$$\begin{bmatrix} u_{AN}(k) \\ u_{BN}(k) \\ u_{CN}(k) \end{bmatrix} = \frac{E}{3} \begin{bmatrix} 2 & -1 & -1 \\ -1 & 2 & -1 \\ -1 & -1 & 2 \end{bmatrix} \begin{bmatrix} S_A(k) \\ S_B(k) \\ S_C(k) \end{bmatrix} \quad (10)$$

where $S_x\,(x = A, B, C)$ represents the switches states,

$$S_x = 0 \iff u_{xN} = 0 \quad et \quad S_x = 1 \iff u_{xN} = E \quad (11)$$

In fixed (α,β) reference frame, stator voltages are represented by equation (12), while in (d,q) reference, they are represented by equation (13):

$$\begin{bmatrix} u_\alpha(k) \\ u_\beta(k) \end{bmatrix} = \frac{2}{3} \begin{bmatrix} 1 & -\frac{1}{2} & -\frac{1}{2} \\ 0 & \frac{\sqrt{3}}{2} & -\frac{\sqrt{3}}{2} \end{bmatrix} \begin{bmatrix} u_{AN}(k) \\ u_{BN}(k) \\ u_{CN}(k) \end{bmatrix} \quad (12)$$

$$\begin{bmatrix} u_d(k) \\ u_q(k) \end{bmatrix} = R(k) \begin{bmatrix} u_\alpha(k) \\ u_\beta(k) \end{bmatrix} = \frac{2}{3} R(k) \begin{bmatrix} 1 & -\frac{1}{2} & -\frac{1}{2} \\ 0 & \frac{\sqrt{3}}{2} & -\frac{\sqrt{3}}{2} \end{bmatrix} \begin{bmatrix} u_{AN}(k) \\ u_{BN}(k) \\ u_{CN}(k) \end{bmatrix} \quad (13)$$

Where $R(k)$ represents the rotation matrix between (α,β) to (d,q) frames.

III. TWO PMSM CONNECTED IN PARALLEL TO ONE INVERTER

The structure is represented in figure 2. There are 2 speed loops, one for each of the machines with a common reference speed ωref = ωr1 = ωr2 since the machines must turn at the same speed. Two PI speed regulators provide the reference torque for each machine, which also depend on the load torque. The control configuration applied to the inverter is unique and built taking into account the data of the two machines to obtain the desired speed, while ensuring the stability of the whole system.

The voltages at the terminals of the two machines are identical in the (α,β) reference frame and the currents prediction in the machines is given by the following relationships:

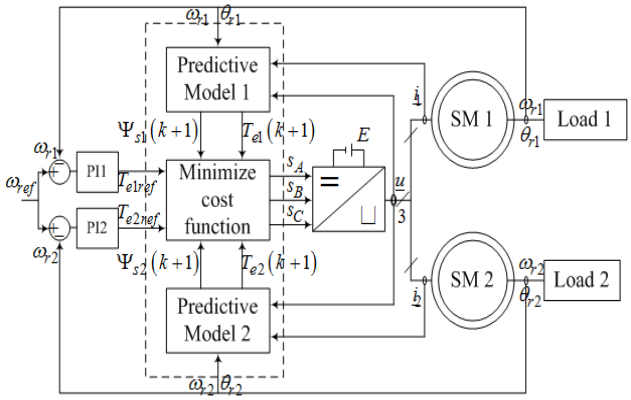

Fig. 2: Mono inverter dual parallel PMSM

$$\begin{bmatrix} i_{d1,d2}(k+1) \\ i_{q1,q2}(k+1) \end{bmatrix} = \begin{bmatrix} 1 - T_s\frac{R_S}{L} & T_s\omega_{r1,r2}(k) \\ -T_s\omega_{r1,r2}(k) & 1 - T_s\frac{R_S}{L} \end{bmatrix} \begin{bmatrix} i_{d1,d2}(k) \\ i_{q1,q2}(k) \end{bmatrix} + \begin{bmatrix} \frac{T_S}{L} & 0 \\ 0 & \frac{T_S}{L} \end{bmatrix} \begin{bmatrix} u_{d1,d2}(k) \\ u_{q1,q2}(k) \end{bmatrix} + \begin{bmatrix} 0 \\ T_S\frac{\omega_{r1,r2}(k)}{L} \end{bmatrix} \Psi_f \quad (14)$$

The voltages at the terminals of the machines in the (d,q) reference can be calculated by (15):

$$\begin{bmatrix} u_{d1,d2}(k) \\ u_{q1,q2}(k) \end{bmatrix} = \begin{bmatrix} \cos\theta_{r1,r2}(k) & \sin\theta_{r1,r2}(k) \\ -\sin\theta_{r1,r2}(k) & \cos\theta_{r1,r2}(k) \end{bmatrix} \begin{bmatrix} u_\alpha(k) \\ u_\beta(k) \end{bmatrix} \quad (15)$$

Where $\theta_{r1,r2}(k)$ represent the electrical angles associated with the positions of each rotor machine. Here, we consider that these two information are measurable and delivered by position sensors. Depending on the chosen control law, the cost function is calculated differently.

Since it is a non-salient pole machine, we impose $i_{dref} = 0$. So, the choice of the control configuration S_x (x = A,B,C) minimizing the cost function, allows imposing the torque while minimizing losses, because the current on the axis d will be the minimum (0). In addition, this control ensures the stability of the synchronous machine [10]. For each criterion (g), predictions are marked by the exponent "p"

CL1:

For this control law, first master and slave machines must be identified. To ensure the stability of the system, it is necessary to control the machine with the highest mechanical load angle. So, to determine the master machine, the electrical positions θ_{r1}, θ_{r2} must be compared. The machine that has the smallest value of this angle will be the master machine [3]. Then, for this master machine, the best control vector is obtained by analyzing the following cost function for all the possible inverter configurations.

$$g = \sqrt{\left(i_{qref} - i_q^p\right)^2 + \left(i_d^p\right)^2} \quad (16)$$

CL2

For this control law the two machines are considered identically and the cost function is evaluated by considering currents on the d and q axis for both machines:

$$g = \sqrt{\left(i_{qref1} - i_{q1}^p\right)^2 + \left(i_{d1}^p\right)^2 + \left(i_{qref2} - i_{q2}^p\right)^2 + \left(i_{d2}^p\right)^2} \quad (17)$$

CL3:

The selected cost function is the same as in CL2 (eq.17). In addition, the obtained control vector serves as a base to look for a better virtual voltage vector, situated in one of the two adjacent sectors of this base solution, which will lead to a lower value of the cost function [16]. That implies using virtual vectors, which will be defined in a finite number, in order to reduce the computational cost of the algorithm. These virtual vectors are characterized by spaced angular positions of Δα=10°, and step amplitudes of ΔV=10 V from 0 to V_{max} ($E/\sqrt{3}$) (Figure 3).

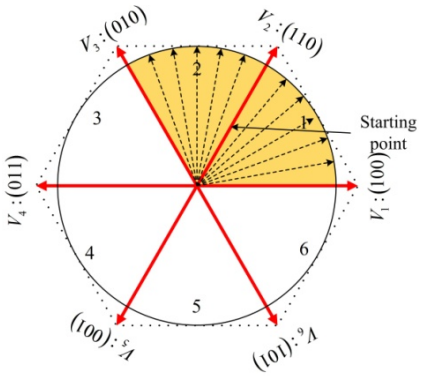

Fig. 3: Representation of the considered virtual vectors.

The research of the best vector consists on a systematic sweep of solutions starting from the evaluation of the cost function for the 7 different control vectors representing the real states of the converter. The vector corresponding to the lower value of the cost function will be chosen (V_2 in figure 3). In a second step, several virtual vectors defined in the two adjacent sectors of the chosen vector, will be evaluated in the cost function. These vectors will be spaced of Δα=10°. That will allow us to determine the angle of the optimum vector to be applied. Next step is calculating the amplitude of this vector. So, virtual vectors, with the same angle than the calculated in the last step, but with different amplitudes, will be tested in the

cost function. These last vectors will be spaced of ΔV=10 V from 0 to V_{max}. The three steps of this algorithm are represented in Figure 4. The total number of vectors to be evaluated in the cost function is 6 in the first step, 10 in the second (5 virtual vectors per sector of 60°) and 30 in the last step, if E=300V. The total number is 6+10+30=46 vectors, which is a relative low number of calculations for the obtained precision. For an equivalent precision in the cost function, and considering directly virtual vectors spaced in the whole control region of the converter, a higher number of calculations must be realized. It can be noted that, in the case of control laws CL1 and CL2, the switching frequency is variable. The commutations are realized when necessary, after each evaluation of the cost function. Meanwhile, control laws CL3 use a modulation technique in order to apply several converter configurations during the same control period. In CL3 method, the calculated virtual vector must be reconstructed from two real control vectors of the converter. In order to make comparisons of the simulation results, the sampling frequency is set to 20 kHz for all the methods, which will correspond to the modulation frequency for method CL3. Better results are expected for control laws working at constant switching frequency, since the others (CL1 to CL2) should be evaluated at higher frequencies (≈ 50 kHz) in order to obtain equivalent precision.

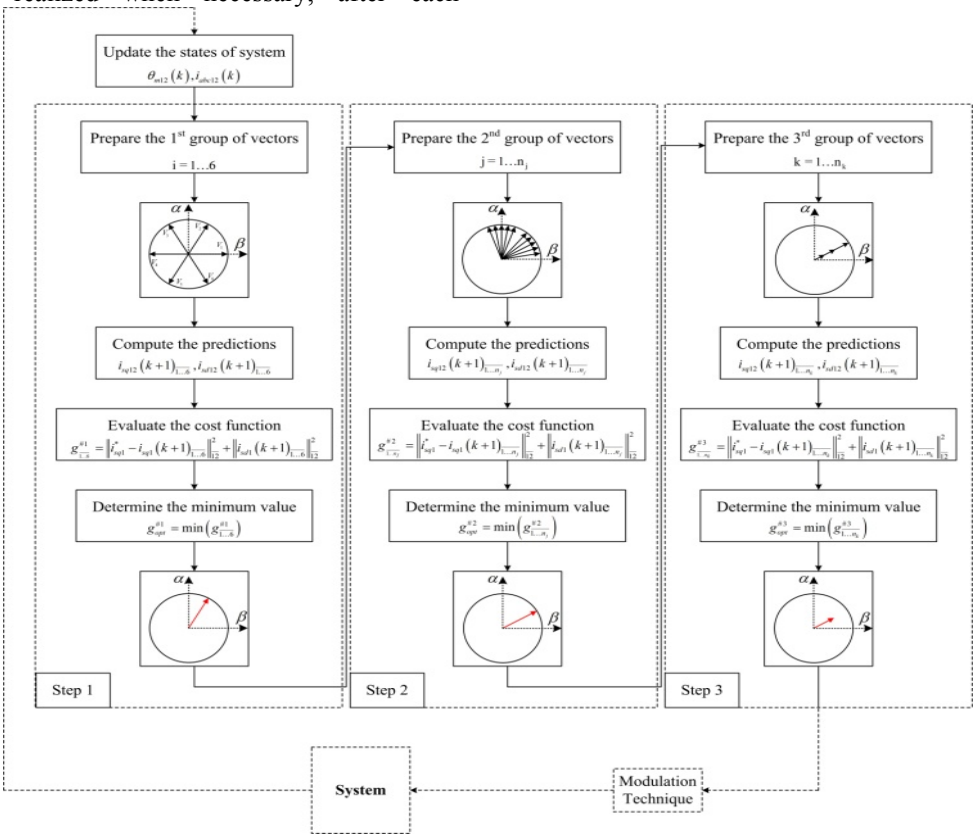

Fig. 4: Block scheme of CL3

IV. TEST PROCEDURE

The different control laws will be compared under a particular load torque profile (figure 5). The comparison is based in two indicators, evaluated over the complete time horizon. The first is used to evaluate the dynamic performance of the control (18) and the second to characterize losses by Joule effect (19), only in the machines.

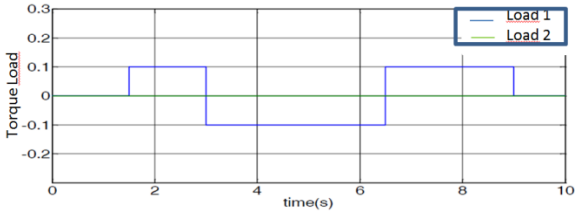

Fig. 5: Reference profile of torque

$$ISE = \sum \left((\omega_{ref} - \omega_{r1})^2 + (\omega_{ref} - \omega_{r2})^2 \right) \Delta t \quad (18)$$

$$Losses_d = R_s . \sum (i_{d1}^2 + i_{d2}^2) . \Delta t \quad (19)$$

Power converter losses are not considered since only the energy efficiency in the PMSM is studied. ISE stands for Integral of Squared Error.

R_s	$2.06(\Omega)$	T_s	$5 \times 10^{-5}(s)$ (20khz)
$L_{sd} = L_{sq} = L$	$9.15 \times 10^{-3}(H)$	T_{emMax}	$5\,N.m$
ψ_p	$0.29(Wb)$	V_{DC}	$540\,V$
Numbers of pole pairs (n_p)	3	Inertia (J)	$7.2 \times 10^{-4}(kg.m^2)$

TABLE II: Parameters for PMSM.

It takes into account the variation of error between the reference and the real values over the whole range of time. Δt is the period of time between the two sampling intervals (T_s here). For the losses by Joule effect, it is considered only the

losses penalties due to the d component of both motor current ($Losses_d$).

V. EXPERIMENTATION PROCESS

The experimental test bench, shown in Fig. 6, includes a system with two PMSM (PMSM1 and PMSM2) connected in parallel to the same inverter. Each motor (800 W) is coupled to its own linear actuator ball screw driven (axis 1 and axis 2) and drives its own slide (slide 1 and slide 2). A third machine (load motor) produces a controlled torque and drives a third slide. This slide is rigidly connected to the slide 1, so that the torque variation can be only applied to PMSM1.

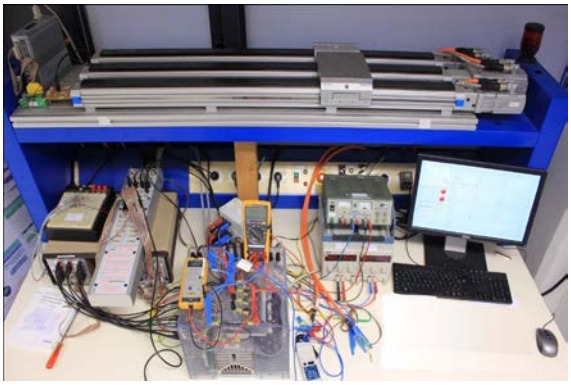

Fig. 6: Experimental setup

First two control laws (CL1, CL2) will lead to variable-frequency operation in power switches, only the sampled time is constant T_s (20 kHz), which does not set the switching frequency. The last control law (CL3) are based in a SVM - PWM modulation at constant switching frequency of 20 kHz. It is important to note the difference between the step calculation and the switching period. Here the values are identical (50 µs) but the switching frequency is not the same for the 3 control laws. When the step calculation is fixed it gives the period of refreshment of the status of the switches and not the switching frequency. Experimental results for the different proposed control methods (CL1 to CL3) are showed next, (Figures 7 to 12).

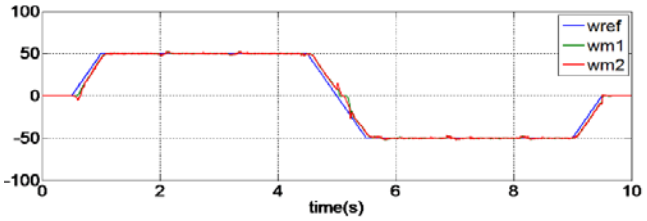

Fig. 7: Speed Rotation (rd/s) – CL1

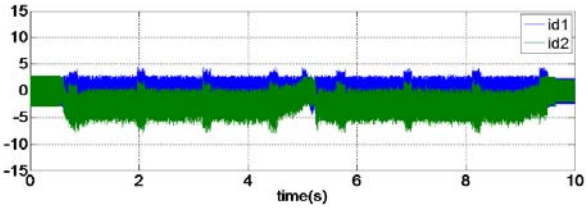

Fig. 8: i_d currents (A) for both PMSM – CL1

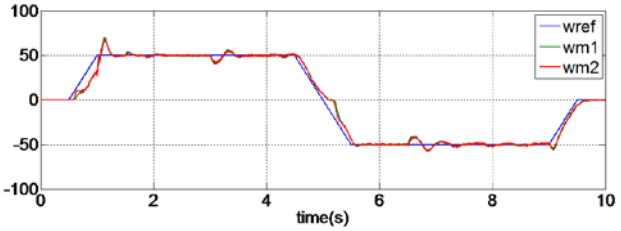

Fig. 9: Speed rotation (rd/s) – CL2

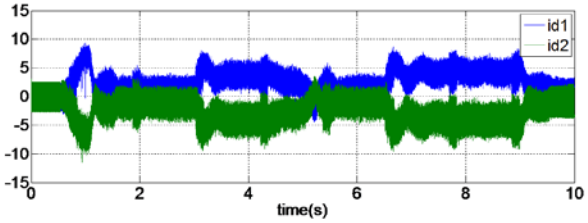

Fig. 10: i_d currents (A) for both PMSM – CL2

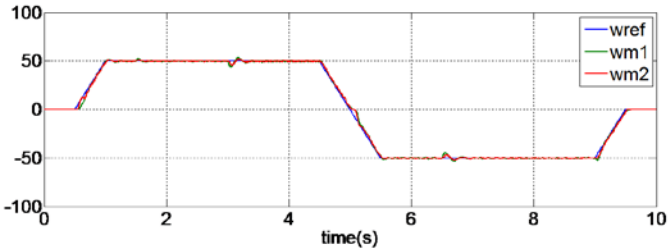

Fig. 11: Speed rotation (rd/s) – CL3

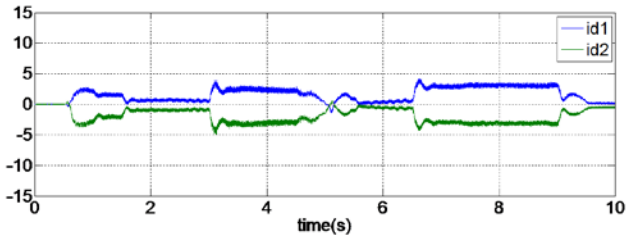

Fig. 12: i_d currents (A) for both PMSM – CL3

From these experimental results, we can conclude that model predictive control is an interesting and powerful solution for the management of the synchronous machines connected in parallel on the same inverter.

	ISE (rd/s)	*$Losses_d$ (J)*
CL1	23.2896	23.8922
CL2	53.2473	45.5072
CL3	8.8425	9.5906

TABLE III: Numerical results for comparison indicators.

The observed behavior depends strongly on the selected cost function. Table III summarizes the results of the 3 control laws giving the numerical values of the indicators. We find that the law of command CL3 guarantees a very good control of the speeds for both machines (the ISE indicator is minimal).″Master-slave″ control solution (CL1) is relatively satisfactory with regard to the ISE test, but presents larger losses (more than 2 times the minimum losses). This is due to the fact that the control law chooses a machine for the torque

control (machine master) and the second machine (slave machine) is still stable but its torque is not directly controlled, so that its d-axis current is no minimal and causes additional losses. CL3 is better from the point of view of ISE and *LossesD*, but since switching losses in the inverter are not considered here, this affirmation must remain cautious. The improvement of CL3 is mainly due to the creation of additional virtual vectors. The control law CL2 shows high values for the two indicators, with a high ISE test and the highest losses. In this case, the decision criterion takes into account the two components of the currents (d and q), so the selected inverter configuration is the result of a compromise for both machines. None of the two reference torques are guaranteed as minimal, leading to higher ISE error and losses.
The consideration of virtual vectors is therefore very effective, allowing building the most suitable voltage vector to minimize the test. The criterion can be still minimized by choosing many more virtual vectors, which will lengthen the procedure for the election of the best control vector. The algorithm proposed in CL3 is a good compromise for the quality of the system response (low current ripple, high dynamic response) and the computation effort required to evaluate the algorithm.

VI. CONCLUSION

Setting two synchronous machines in parallel connected to the same inverter reduces the embedded electronics, and so weight and volume are also reduced. However this power structure shows a stability problem as well as low efficiency of the energy conversion. For this purpose, the predictive control offers various solutions, with control laws acting on predetermined indicators. Three different control laws have been tested, minimizing different cost functions in order to improve the energy efficiency. The voltage inverter gives, at each moment, a voltage (amplitude and phase) which may not be optimal for each of the machines and therefore this opens the way for the optimization. In this sense, a control law using a finite number of virtual vectors, allows the system reaching a minimum of the cost function lower than with classical algorithms. This method still allows reducing the value of the criterion in choosing a higher number of virtual vectors which will increase the calculation time. This solution has the characteristics of a PWM control and the dynamic performances of the predictive control. This is a good compromise for our system. Additional studies are ongoing to take into account losses in the inverter.

VII. REFERENCES

[1] E. Foch, G. Bisson, P. Maussion, M. Pietrzak-David, and M. Fadel, "Power system comprising several synchronous machines synchronously self-controlled by a converter and control method for such a system, " *US Patent, US 2007/0273310 A1,* November 2007.

[2] N.L.Nguyen, M. Fadel, A. Llor, "Predictive Torque Control – A solution for mono inverter-dual parallel PMSM system", *IEEE International Symposium on Industrial Electronics (ISIE)*, June 2011.

[3] D. Bidart, M. Pietrzak-David, P. Maussion, and M. Fadel, "Mono inverter dual parallel PMSM – Structure and control strategy", *IECON 2008, 34th Annual Conference of IEEE,* November 2008.

[4] Mino-Aguilar, G. et al, "A direct torque control for a PMSM", *Electronics, Communications and Computer (CONIELECOMP), 2010 20th International Conference*, 22-24 Feb. 2010.

[5] Miranda, H. Yuz, J. Cortes, P. Rodriguez, J, "Predictive torque control of induction machine based on state space models", *IEEE Transactions on Industrial Electronics, 56(6):1916-1924*, June 2009.

[6] Correa, P.Rivera, M. Rodriguez, J. Espinoza, J. Kolar, J, "Predictive control of an indirect matrix converter", *IEEE Transactions on Industrial Electronics, 56(6):1847-1853*, June 2009.

[7] F. Morel, X. Lin-Shi, J.M. Retif, B. Allard, "A comparative study of two predictive current control for a permanent magnet synchronous machine drive," *Power Electronics Specialists Conference (PESC'08),* June 2008

[8] T. Geyer, G. Papafotiou, M. Morari, "Model Predictive Direct Torque Control – Part I: Concept, Algorithm, and Analysis," *Industrial Electronics, IEEE Transactions,* June 2009.

[9] G. Papafotiou, J. Kley, K.G. Papadopoulos, P. Bohren, M. Morari, "Model Predictive Direct Torque Control – Part II: Implementation and Experimental Evaluation," *IEEE Transactions on Industrial Electronics,* June 2009.

[10] Rodriguez, J. et al, "Speed control of a permanent magnet synchronous motor using predictive current control", *Enegy Conversion Congress & Expo., ECCE (2009, USA)*, 20-24 September 2009.

[11] A. M. Llor, "Commande directe de couple à fréquence de modulation constante des moteurs synchrones à aimants permanent," *Doctoral dissertation, Laboratoire de recherche : CEGELY site INSA de LYON*, April 2003.

[12] S. Hassaine, S. Moreau, C. Ogab, B. Mazari, "Robust Speed Control of PMSM using Generalized Predictive and Direct Torque Control techniques," *IEEE International Symposium* (*ISIE' 07),* 4-7 June 2007.

[13] J. Rodriguez et al, "Model Predictive Control with Constant Switching Frequency Using a Discrete Space Vector Modulation with Virtual State Vector," *IEEE International Conference on Industrial Technology (ICIT' 09)*, 10-13 Feb 2009.

[14] J. Restrepo, J. Viola, J.M. Aller and A. Bueno, "A Simple Switch Selection State for SVM Direct Power Control," *IEEE International Symposium on Industrial Electronics (ISIE'06)*, Montreal, Canada, 9-13 July 2006.

[15] D. Casadei, G. Serra and A. Tani, "Improvement of direct torque control performance by using a discrete SVM technique," *IEEE Power Electronics Specialist Conf. (PESC' 98)*, May 1998

[16] Ngoc Linh Nguyen ; Fadel, M. ; Llor, A, *A new approach to Predictive Torque Control with Dual Parallel PMSM system* , Industrial Technology (ICIT), 2013 , Page(s): 1806 - 1811

[17] E.F Camacho and C. Bordons, *Model Predictive Control*, New York, N.Y, Springer-Verlag, 1999.

[18] Predictive Control of Power Converters and Electrical Drives Jose Rodriguez, Patricio Cortes, Wiley-IEEE 9 April 2012

[19] Jean-Paul LOUIS, Control of Synchronous Motors - Edition Wiley-ISTE ISBN: 9781848212732 April 2011